Journal of Power Sources 193 (2009) 130–135

Contents lists available at ScienceDirect

Journal of Power Sources

journal homepage: www.elsevier.com/locate/jpowsour

Evaluation of the redox stability of segmented-in-series solid oxide fuel cell stacks

K. Fujita*, T. Somekawa, K. Horiuchi, Y. Matsuzaki

Product Development Dept., Tokyo Gas Co., Ltd., 3-13-1 Minami-senjyu, Arakawa-ku, Tokyo 116-0003, Japan

ARTICLE INFO

Article history:
Received 3 October 2008
Received in revised form
13 November 2008
Accepted 13 November 2008
Available online 3 December 2008

Keywords:
Solid oxide fuel cell
Redox
Segmented-in-series

ABSTRACT

The tolerance for the reduction and oxidation (redox) reactions of the segmented-in-series solid oxide fuel cells (SIS-SOFCs) has been investigated. In conventional anode-supported solid oxide fuel cells (SOFCs), the anode and the substrate are typically prepared from Ni–YSZ-based materials which exhibit a significant dimensional change because of the redox reaction and cannot retain their structure. The substrate of the SIS-SOFCs is prepared from Ni-doped MgO-based material, which has a high redox tolerance, and the SIS-SOFC exhibits a good performance after the redox cycles.

The degradation rate is approximately 0.15% per cycle in a redox condition of start-and-stop operation without fuel supply. In the other redox condition (when the fuel supply is interrupted for 1.5 min), the voltage of the SIS-SOFCs remains almost constant. However, the voltage of SIS-SOFCs decreases with an increase in the reoxidation time of the interruption in the fuel supply. The high redox tolerance is attributed to the fact that the diffusion coefficients, mean free path, and existence of the Ni particles in the substrate can effectively deter the oxidation of the anode.

1. Introduction

Redox tolerance in a small-scale solid oxide fuel cell (SOFC) system is considered important for the practical applications of the system. In the case of a reliable SOFC system, a high redox durability gives some advantages such as temporary high fuel utilization stability and emergency shutdown without any reduction in the purge gas.

The redox mechanism for the anode in SOFCs has been studied by many researchers in order to enhance the redox tolerance of the cells [1–4]. Further, the redox degradation has been attributed to the microstructural changes in the nickel–yttria-stabilized zirconia (Ni–YSZ) anode. The substrate of the anode-supported fuel cells (ASCs), which was typically prepared by using Ni–YSZ cermet, exhibits a significant dimensional change and is responsible for the formation of cracks in the electrolyte and the substrate. Therefore, it is important to devise a method for preventing the oxygen from flowing into the anode.

We developed segmented-in-series solid oxide fuel cells (SIS-SOFCs) in 2003 [5,6]. The stack of the SIS-SOFCs resembled a flattened tube, and the 16 single cells were connected electrically in series by using ceramic interconnects on a porous substrate; the substrate was made of an insulating material. A schematic representation of an SIS-SOFC is shown in Fig. 1; the stack design was determined through numerical analyses [7–9]. The above-mentioned electrically insulating substrate was prepared from a Ni-doped MgO-based material, and the stability of this substrate was examined [10,11]. The dimensional stability, the small structural change, and the small residual stress change in the electrolyte were confirmed in the redox cycle. In this study, we have examined the redox cycle and the redox tolerance of an SIS-SOFC.

2. Experimental

2.1. SIS-SOFC preparation

The SIS-SOFC fabrication method comprises five major processes: extrusion, tape casting, dip coating, cofiring, and screen printing. The electrically insulating substrate is prepared from a Ni-doped MgO-based material, and extruded in the form of a flattened tube. The anode is prepared from well-mixed NiO powder (99.9%, Seido Chemical Industry Co., Ltd.) and 8 mol% YSZ powder (TZ-Y, Toso Co., Ltd.). The anode sheets are produced by using a tape casting method and arrayed on the substrate. Then, the substrate with the anode is dipped in a YSZ slurry, and the YSZ electrolyte is cofired with the substrate and the anode. Next, the cathode of Sr- and Co-doped $LaFeO_3$ (LSCF) is screen printed on the electrolyte and sintered. Samples of the electrolyte and the cathode are prepared by using almost the same method as that reported in our previous papers on ASCs [12,13].

* Corresponding author. Tel.: +81 3 5604 8275; fax: +81 3 5604 8051.
E-mail address: k-fujita@tokyo-gas.co.jp (K. Fujita).

0378-7753/$ – see front matter © 2008 Elsevier B.V. All rights reserved.
doi:10.1016/j.jpowsour.2008.11.091

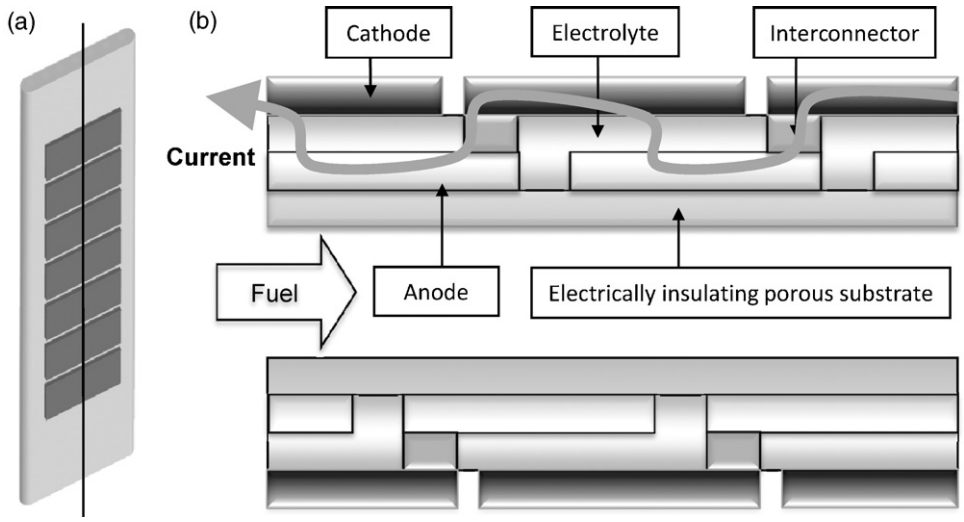

Fig. 1. Schematic representation of (a) the plane view and (b) the cross-sectional view of the SIS-SOFC.

Table 1
The procedure of the start-and-stop operation without the reducing gas supply.

Step	T_{start} (°C)	T_{end} (°C)	Time (h)	Inlet gas composition on fuel side	Process
1. Heating	20	300	1.2	Air: 0.91 $cm^3\ min^{-1}$	Reoxidation
2. Heating	300	700	1.3	Air: 0.91 $cm^3\ min^{-1}$, H_2O: 1.63 $\mu l\ min^{-1}$	Reoxidation
3. Heating	700	775	0.5	CH_4: 2.17 $cm^3\ min^{-1}$, H_2O: 4.00 $\mu l\ min^{-1}$	Reduction
4. Hold	775	775	0.4	CH_4: 5.02 $cm^3\ min^{-1}$, H_2O: 9.25 $\mu l\ min^{-1}$	IV
5. Cooling	775	700	0.5	CH_4: 2.17 $cm^3\ min^{-1}$, H_2O: 4.00 $\mu l\ min^{-1}$	Reduction
6. Cooling	700	300	3	Air: 0.91 $cm^3\ min^{-1}$, H_2O: 1.63 $\mu l\ min^{-1}$	Reoxidation
7. Cooling	300	20	>10	Air: 0.91 $cm^3\ min^{-1}$	Reoxidation

2.2. SIS-SOFC stack performance

The current–voltage (*I–V*) and current–power characteristics of the SIS-SOFC stack were measured at 775 °C when steam-reformed methane (S/C = 2.5) was used as the fuel. Further, durability and thermal cycle stability tests were conducted for obtaining baseline data.

The redox tolerance of an SIS-SOFC was estimated by using two different redox conditions. The first condition was a start-and-stop operation that did not involve using a reducing gas as the purge gas. For completely replacing the residual gas in the experimental pipes, air was supplied as the oxidation gas to the anode side of the cell. The oxidation process of the SIS-SOFC was carried out in a furnace with dry air at temperatures of up to 300 °C and with humidified air at temperatures of up to 700 °C. A reduction reaction was carried out by using steam-reformed methane (S/C = 2.5) from 700 to 775 °C for 30 min, and then the open-circuit voltage (OCV) and *I–V* characteristics were measured under the same fuel and temperature conditions. After the measurements, the SIS-SOFC was cooled down to room temperature in a reoxidation atmosphere. This thermal cycle test along with the redox reaction was carried out 20 times; refer to Table 1 for further details.

Next, a redox examination by using a fuel flow interrupt technique was performed at 775 °C. After measuring the *I–V* characteristics, we carried out the reoxidation process by supplying humidified air for 1.5 min before supplying the reformed methane. The performances after each redox cycle were evaluated by mea-

Table 2
The procedure of the fuel flow interrupt method.

	Process	Time (min)	Inlet gas composition on fuel side		
			CH_4 ($l\ min^{-1}$)	H_2O ($\mu l\ min^{-1}$)	Air ($l\ min^{-1}$)
1	First reoxidation	1.5	0	1.63	0.91
	Reduction IV measurement		0.502	9.25	0
2	Second reoxidation	10	0	1.63	0.91
	Reduction IV measurement		0.502	9.25	0
3	Third reoxidation	15	0	1.63	0.91
	Reduction IV measurement		0.502	9.25	0
4	Fourth reoxidation	20	0	1.63	0.91
	Reduction IV measurement		0.502	9.25	0
5	Fifth reoxidation	25	0	1.63	0.91
	Reduction IV measurement		0.502	9.25	0
6	Sixth reoxidation	30	0	1.63	0.91
	Reduction IV measurement		0.502	9.25	0

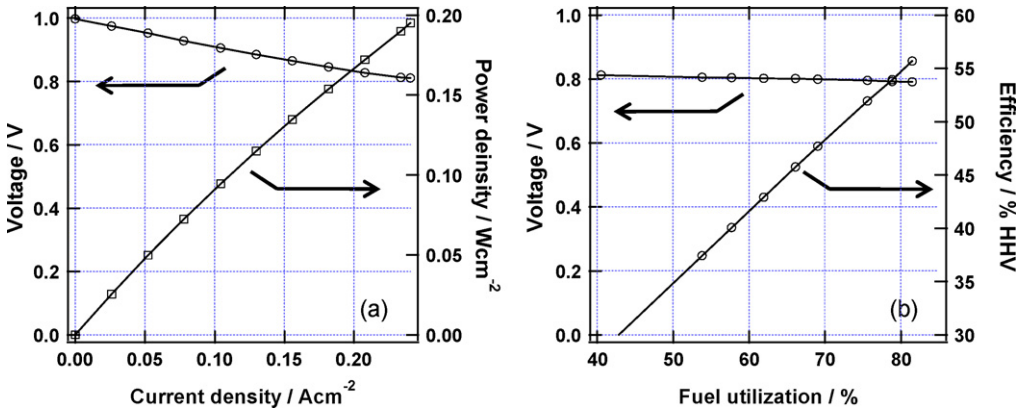

Fig. 2. (a) Current–voltage and power density characteristics and (b) fuel utilization dependences of an average cell-stack voltage and electrical efficiency of the segmented-in-series SOFC stack with a fuel of steam-reformed methane (S/C = 2.5) at 775 °C.

suring the OCV, *I–V*, and IR characteristics. The IR characteristics were measured using a current-interruption method. The redox procedures are given in Table 2.

After these measurements, the anode and the substrate of the SIS-SOFC stack were analyzed by using a scanning electron microscope (SEM, JEOL Ltd., EX-23000BU).

3. Results and discussion

Fig. 2 shows (a) the *I–V* characteristics and (b) the fuel utilization dependence of the SIS-SOFC stack voltage as baseline data before the redox cycles. The average stack power density when reformed methane was used as the fuel was 0.195 W cm^{-2} at 0.24 A cm^{-2} at Uf = 35%. A conversion efficiency of 53.9% HHV was obtained at an average voltage, an output power, a current density, and a Uf of 0.79 V, 0.19 W cm^{-2}, 0.24 A cm^{-2}, and 78.9%, respectively. Figs. 3 and 4 show the SIS-SOFC durability performances as a function of the elapsed time and the thermal cycle; durability rates of 0.28%/1000 h and 0.12% per cycle were obtained under normal conditions.

The performances were examined after the start-and-stop operation mentioned earlier. The obtained OCV and the average cell voltage at a current density of 0.24 A cm^{-2} are shown in Fig. 5. The OCV remained almost constant, and the voltage

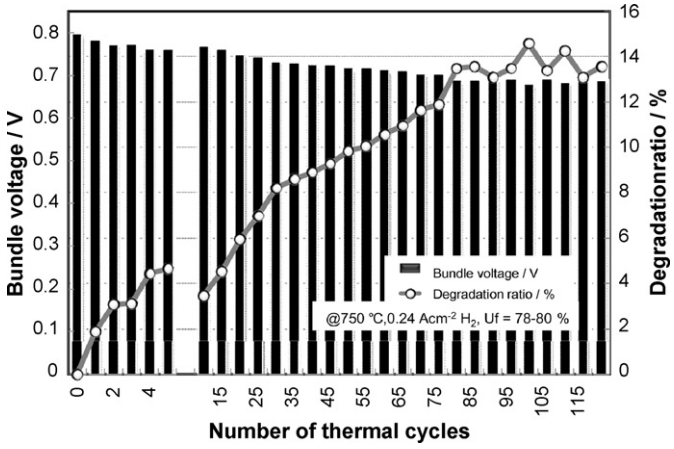

Fig. 4. Thermal cycle test results of the SIS-SOFC at 0.2 A cm^{-2} at 750 °C.

decreased slightly; the degradation ratio of the redox cycles was approximately 0.15% per cycle. This ratio was almost the same as that of the durability of the normal start-and-stop operation. The high durability of the SIS-SOFC shows the possibility of developing such a system without using a purge gas. The

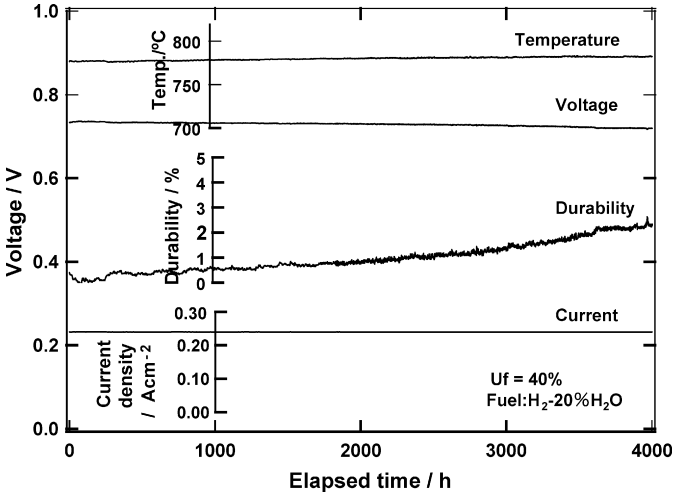

Fig. 3. Durability test results of the SIS-SOFC at 0.2 A cm^{-2} at 775 °C.

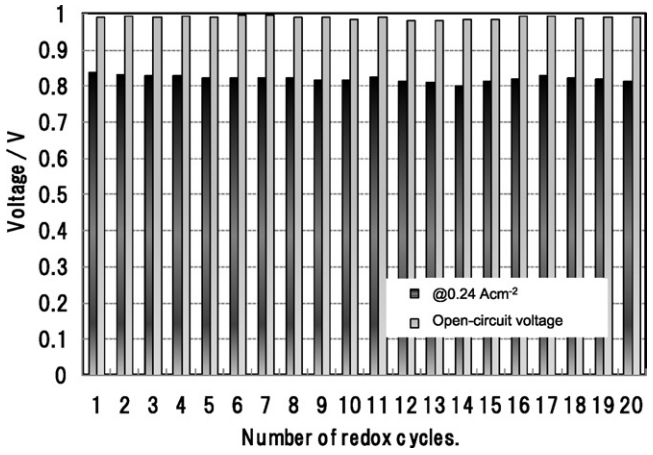

Fig. 5. SIS-SOFC performance after the start-and-stop operation without the reducing gas supply.

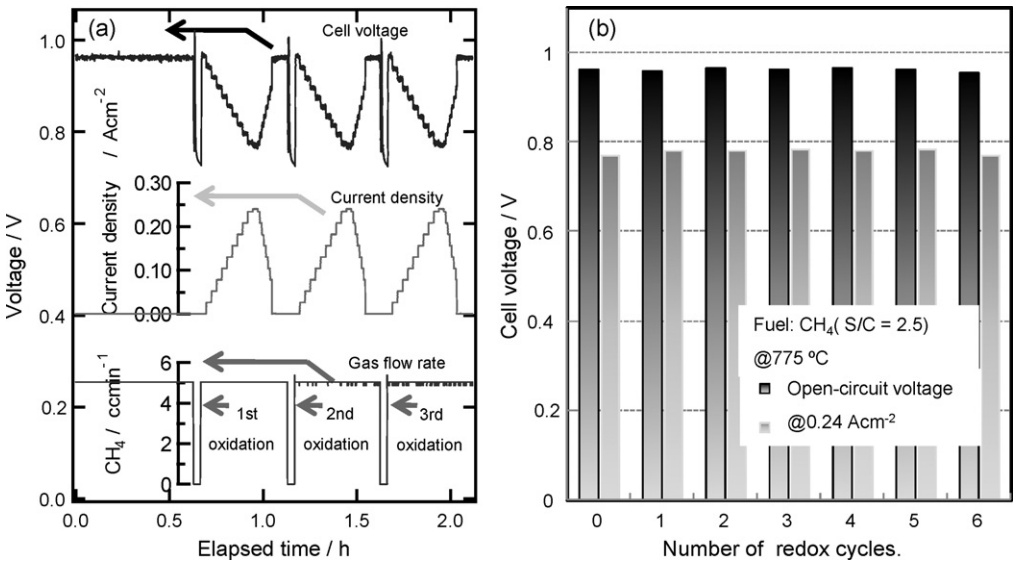

Fig. 6. SIS-SOFC performance after fuel flow interrupt operation: (a) voltage behavior during the fuel interrupt redox cycles and (b) OCV and voltage after redox cycles.

OCV during the start-up period increased at temperatures above 400 °C, and attained the value of approximately 0.8 V before the reformed methane was supplied at around 700 °C. The OCV during the shutdown process exhibited almost the same behavior. This implies that the partial pressure of oxygen in the anode remains constant when air was supplied to the anode side fuel channel.

Next, the voltage of the SIS-SOFC was measured after the flow of the reducing fuel was interrupted for 1.5 min. The OCV decreased rapidly from approximately 1.0 V and remained constant at approximately 0.8 V (see Fig. 6(a)). The *I–V* characteristics were obtained at 775 °C after a rereduction with the steam-reformed gas (S/C = 2.5). The voltage at 0.24 A cm^{-2} remained almost constant during the redox cycles, as shown in Fig. 6(b). However, the voltage decreased with an increase in the reoxidation time. The time dependence of the OCV, voltage, and IR are shown in Fig. 7. The voltage decreased with an increase in the IR. The degradation rate of the voltage was approximately 6.6% h^{-1} and the increase rate of ohmic resistance, approximately 3.5% h^{-1}. The increase in IR was attributed to the progressive oxidation of the anode with an increase in the reoxidation time. An OCV value of less than 0.03 V was confirmed after oxidation for 30 min. The oxygen partial pressure in the anode was almost the same as that at the cathode side, and it was easy to oxidize the Ni in the anode to NiO. However, we confirmed that the SIS-SOFC was able to successfully generate electricity only after the redox cycles.

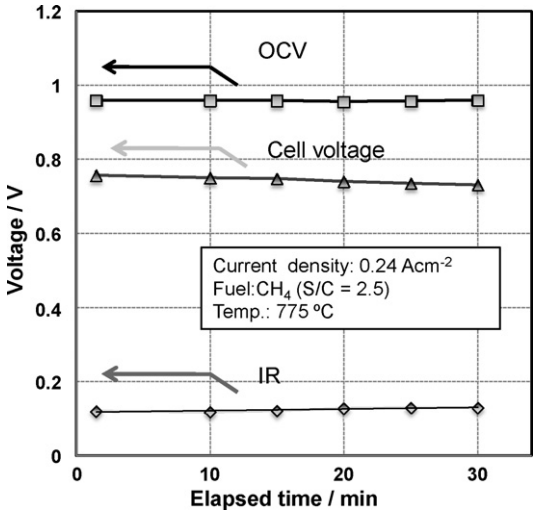

Fig. 7. SIS-SOFC performance as a function of fuel flow interrupted time. The IR characteristics were measured by using current interrupt method.

The SEM images of the anode after the start-and-stop operation and the fuel flow interrupt operation are shown in Fig. 8(a) and (b), respectively. The SEM images of an oxidized sample, which was annealed in the furnace at 800 °C for 1 h, are shown in Fig. 8(c) for reference. The anodes after the redox cycles still had the reducing morphology of the Ni–YSZ cermet in which NiO was hardly observed, as in the case of the reference samples. However, a different morphology was observed in the restrictive area, which was shown in Fig. 8(d). The partially confirmed morphology was attributed to the NiO particles, and the anode was found to be partially exposed in the oxidation environments.

Fig. 9(a) and (b) shows the SEM image of the substrate, and Ni particles were identified in the grain boundaries. However, another area in which the Ni particles were not seen was observed, and the SEM image of this area is given in Fig. 9(d). This morphology was similar to that of the annealed reference substrate shown in Fig. 9(c). These results show that the reduction reaction was more dominant in the substrate although a partial oxidation atmosphere did exist.

The SIS-SOFC stack had an electrically insulating porous substrate, which was located between the fuel channel and the anode, as shown in Fig. 1. It was considered that the substrate functioned as an oxidation barrier layer that prevented the oxidation gas from coming in direct contact with the anode. Thus, the OCV was obtained without supplying fuel for few dozens of minutes since the substrate could deter the diffusion of oxygen. The oxidation deterrence effect was attributed to not only the diffusion coefficient of the substrate but also the Ni particles in the substrate. Even if the anode oxidized partially, the amount of structural change was smaller than that observed in the case of general ACSs, and the SIS-SOFC exhibited a high redox tolerance.

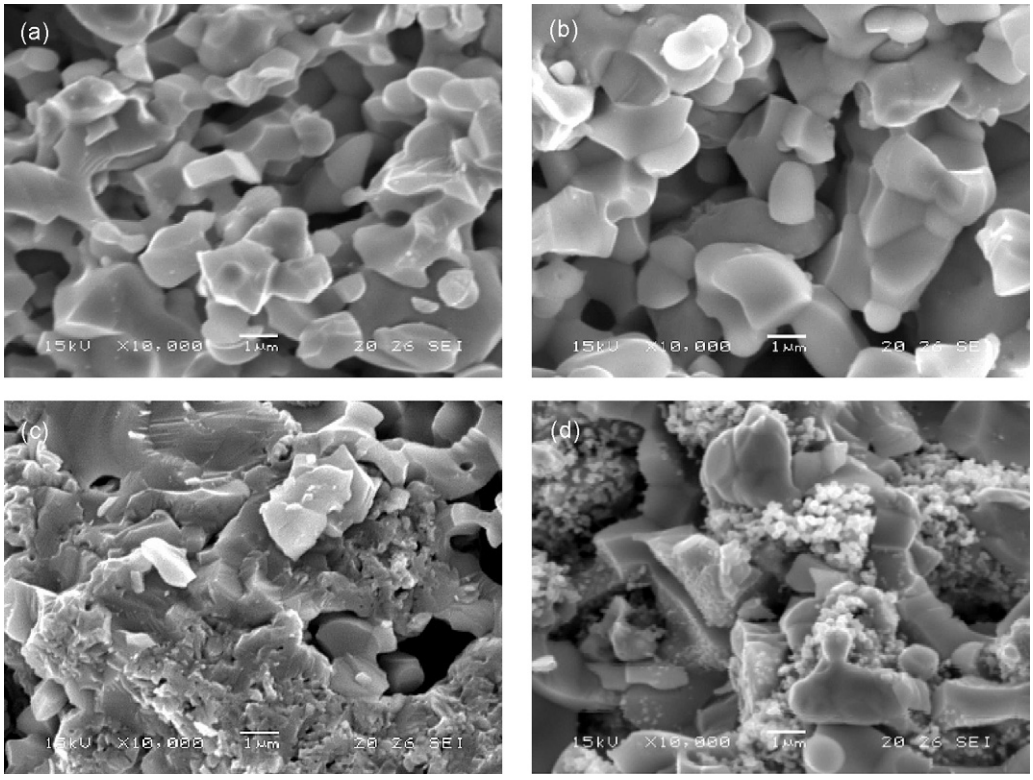

Fig. 8. SEM images of the anode: (a) after the start-and-stop operation without the reducing gas supply, (b) after the fuel flow interrupt operation, (c) after annealing in the furnace at 800 °C for 1 h for reference and (d) a partially oxidized morphology observed in the restrictive area.

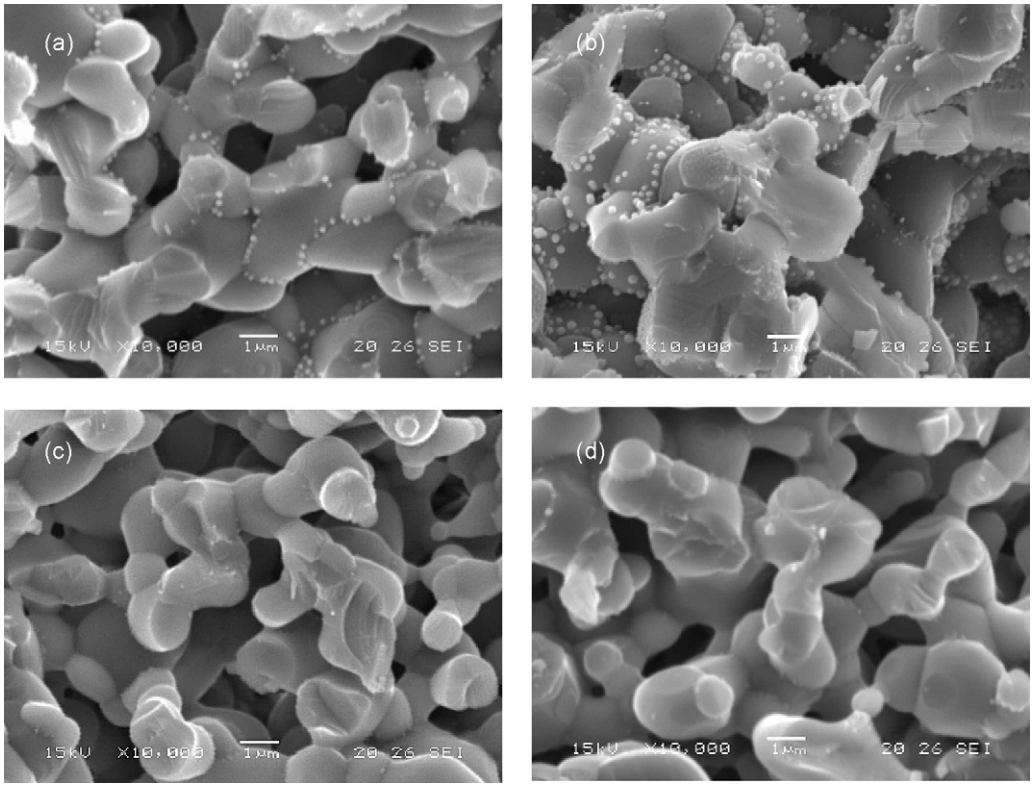

Fig. 9. SEM images of the substrate: (a) after the start-and-stop operation without the reducing gas supply, (b) after the fuel flow interrupt operation, (c) after annealing in the furnace at 800 °C for 1 h for reference and (d) a partially oxidized morphology observed in the restrictive area.

4. Conclusion

The SIS-SOFC exhibited a high tolerance for redox cycles. Degradation rates of approximately 0.15% per cycle and 6.6% h^{-1} were obtained in the start-and-stop operation without fuel supply and the fuel flow interrupted operation, respectively. The high redox tolerance was attributed to the fact that the diffusion coefficients, the mean free path, and the existence of the Ni particles in the substrate could effectively deter the oxidation of the anode, and the thin anode exhibited only a slight dimensional change as compared to that observed in the case of conventional anode-supported SOFCs. Therefore, because of its high redox tolerance, the SIS-SOFC system is suitable for small-scale power generation systems that do not have a purge gas supply.

References

[1] D. Sarantaridis, R.J. Chater, A. Atkinson, J. Electrochem. Soc. 155 (2008) B467–B472.
[2] D. Waldbillig, A. Wood, D.G. Ivey, J. Electrochem. Soc. 154 (2007) B133–B138.
[3] T. Kemenso, C.C. Appel, M. Mogensen, Electrochem. Solid State Lett. 9 (2006) A403–A407.
[4] A. Wood, M. Pastula, D. Waldbillig, D.G. Ivey, J. Electrochem. Soc. 153 (2006) A1929–A1934.
[5] M. Koi, S. Yamashita, Y. Matsuzaki, ECS Trans. 7 (2007) 235–243.
[6] Y. Matsuzaki, M. Koi, S. Yamashita, Proceedings of 2nd European Fuel Cell Technology and Applications Conference (EFC 2007), Rome, Italy, December 11–14, 2007, pp. 153–154.
[7] K. Fujita, Y. Matsuzaki, H. Yakabe, S. Yamashita, K. Ogasawara, T. Sakurai, Proceedings of 4th International ASME Conference on Fuel Cell Science Engineering and Technology (FuelCell 2006), Irvine, CA, USA, June 19–21, 2006 (on CD).
[8] H. Yakabe, ECS Trans. 7 (2007) 347.
[9] H. Yakabe, K. Fujita, T. Sakurai, ECS Trans. 1 (2006) 1.
[10] K. Horiuchi, T. Somekawa, Y. Matsuzaki, M. Nishihara, Proceedings of 2nd European Fuel Cell Technology and Applications Conference (EFC 2007), Rome, Italy, December 11–14, 2007, pp. 155–156.
[11] T. Somekawa, K. Horiuchi, Y. Matsuzaki, M. Nishihara, S. Inoue, S. Yamashita, Proceedings of 31st International Cocoa Beach Conference & Exposition on Advanced Ceramics & Composites, Daytona Beach, FL, USA, January 21–28, 2007, pp. 167–168.
[12] Y. Matsuzaki, Y. Baba, T. Sakurai, Solid State Ionics 174 (2004) 81–86.
[13] Y. Matsuzaki, Y. Baba, T. Ogiwara, H. Yakabe, Proceedings of 5th European SOFC Forum, Lucerne, July 2002, p. 776.